Rational engineering of dimeric Dy-based Single-Molecule Magnets for surface grafting

Xiaohui Yi, Fabrice Pointillart, Boris Le Guennic, Julie Jung, Carole Daiguebonne, Guillaume Calvez, Olivier Guillou, Kevin Bernot

Rational engineering of dimeric Dy-based single-molecule magnets for surface grafting

Xiaohui Yi,[a] Fabrice Pointillart,[a] Boris Le Guennic,[a] Julie Jung,[a,b] Carole Daiguebonne,[a] Guillaume Calvez,[a] Olivier Guillou[a] and Kevin Bernot*[a]

[a] Univ Rennes, INSA Rennes, CNRS, ISCR (Institut des Sciences Chimiques de Rennes) – UMR 6226, F-35000 Rennes, France

[b] Los Alamos National Laboratory, Theoretical Division, Los Alamos, NM 87545, USA

Corresponding author: Kevin.bernot@insa-rennes.fr (K. Bernot)

Dedicated to Professor Miguel Julve on the occasion of his 65th birthday, and for its outstanding contribution to the field of coordination chemistry and molecular magnetism.

Abstract

The deposition of Single-Molecule Magnets (SMMs) on surfaces is a mandatory step toward their possible use as data-storage units or qubits. In this study we report the structural and magnetic characterization of two parent compounds of a well-known SMM called **DyPyNO**, ([Dy(hfac)$_3$(PyNO)]$_2$ with hfac = hexafluoroacetylacetonate and PyNO = pyridine-N-oxide), that are targeted to be deposited on gold surfaces. Thio-substitution of the pyridine ring of these dimers is expected to provide good anchoring group toward deposition on gold. We have investigated two significantly different geometries of the anchoring groups in dimers **1** and **2**. Interestingly, despite these strong differences, SMM behavior is remarkably well-preserved in the polycrystalline material offering possibilities to graft these SMMs on surface.

Keywords

Lanthanides, Sulfured ligands, Single-Molecule Magnets, Dimers, Electrostatics, Surface.

1. Introduction

Single-molecule magnets (SMMs) are molecules able to act as magnets at the molecular scale.[1, 2] Their unique magnetic behavior can be used in functional devices, mainly in the field of low-temperature molecular magnetic data storage.[3-6] The exploitation of SMMs in this area of research requires being able to assemble them in ordered arrays, where each bit of information can be easily addressed. Thus technological applications with SMMs as key molecular components will require the formation of monolayer or thin film coverage on adapted substrates. The two main routes to do so are physical [7] or chemical deposition. [8, 9] The latter is possibly more adapted to the formation of monolayers because on-surface auto-organization of the molecules can occur. Such self-assembled monolayers (SAM) of SMMs were mainly reported on molecules functionalized by thio-methyl groups in order to graft them on Au(111) surfaces.[10-13]

Some of us previously reported a series of Dy-based SMMs (called **DyPyNO**)[14] that can be physic-sorbed as thick-films on surfaces by sublimation techniques.[15] Chemical tuning of this molecular platform allows to organize the SMMs in a 3D molecular material,[16] to optimize their SMM behavior by ligand substitution[17, 18] and to transfer this enhancement on molecular thick films.[18] It also allows to test their dependence toward Dy^{III} isotopic substitution [17] and even to produce devices with electric driven reversible luminescent modulation.[19]

In order to deposit **DyPyNO** as SAM on gold it has to be substituted by thio-based groups. However, the magnetic behavior of lanthanide-based SMMs is extremely sensitive to small geometric molecular changes.[5, 20-30] The objective of this work is to study the possibility of thio-substitution of **DyPyNO** and the influence on its SMM behavior.

Two different ligands were used, with different length and orientation of the anchoring groups that may provide different grafting ability. First one is 3-methylsulfanyl-pyridine N-oxide (**L1**) and reaction with $[Dy(hfac)_3(H_2O)_2]$ ($hfac^-$ = hexafluoroacetylacetonate) provides $[Dy(hfac)_3(\mathbf{L1})_2]_2$, latter called **1**. The second one is 4-methylcarbodithioate-pyridine N-oxide (**L2**) and provides $[Ln(hfac)_3(\mathbf{L2})_2]_2$ latter called **2**. This ligand may

induce stronger sulfur bonding with the gold surface (two available sulfur atoms) as well as an enhanced spacing between the gold surface and the $hfac^-$ ancillary ligands.

2. Materials and methods

Reagents: All other reagents were purchased from Aldrich Co., Ltd. and used without further purification.

X-ray crystallography: Single crystals of **1** and **2** were mounted on APEXII AXS Bruker diffractometer form CDIFX (ISCR diffractometry center). It is equipped with a CCD camera and a graphite monochromated Mo-Kα radiation source (λ = 0.71073 Å). Data were collected at 150K. Structure solving was done via direct methods using SIR-97 [31] and refined trough WinGX interface [32] using SHELXL program.[33] Crystallographic data can be found in supplementary materials. All data were deposited to the Cambridge Structural Data Base under CCDC 1819460 and CCDC 1819461 for **1** and **2**, respectively.

NMR: ^{1}H NMR spectra were recorded with a Bruker Ascend 400 spectrometer. Chemical shifts are reported in parts per million referenced to TMS for ^{1}H NMR spectroscopy.

Powder X-ray diffraction: X-ray powder diffractogramms were collected using a Panalytical X'Pert Pro diffractometer equipped with an X'celerator detector in θ-θ mode with Cu-Kα (λ = 1.54 Å). The calculated patterns were produced using Mercury 3.0 (Figure S1).

TGA/TDA analysis: Analyses were performed using a PerkinElmer Pyris Diamond thermal analyzer with a 5°C/min heat rate under N_2 atmosphere (100mL.min^{-1})

Magnetic measurements: Static and dynamic magnetic measurements were performed on single-crystals picked one by one in the preparation mixtures. They were then ground and pressed in pellets to avoid crystallite orientations. Measurements were performed on a Quantum design MPMS magnetometer equipped with a RSO

probe. All measurements were corrected from the contribution of the sample holders and their diamagnetic contribution subtracted according to Pascal's constants.

Ab-initio calculations: Wavefunction-based calculations were carried out on **1** and **2** by using the SA-CASSCF/RASSI-SO approach, as implemented in the MOLCAS quantum chemistry package (see SI for more details).

3. Experimental

Precursor synthesis: $Dy(hfac)_3(H_2O)_2$ precursor were synthesized according to reported methods.[34]

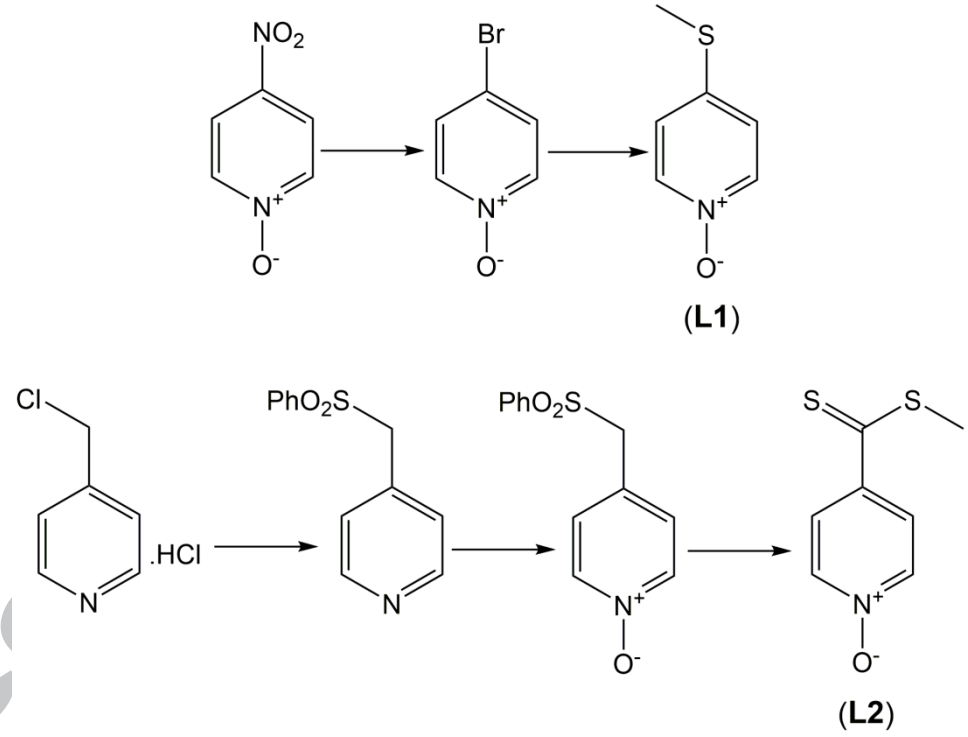

Scheme 1. Synthetic scheme for the design of **L1** and **L2**.

3-methylsulfanyl-pyridine N-oxide (L1): 420 mg of 3-nitropyridine-N-oxide were placed in 2 mL of acetic acid. 3.6 mL of acetyl bromide are added. After 3h of stirring at 80°C, the mixture is cooled at room temperature and then put in ice before neutralization with NaOH 10 M then Na_2CO_3. The aqueous phase is extracted four times with CH_2Cl_2. The organic phases are combined then dried with $MgSO_4$. After

evaporation of the organic solvent under vacuum, the resulting 3-bromopyridine-N-oxide powder is used for the next step without further purification (Yield: 452 mg, 87 %). The 452 mg of 3-bromopyridine-N-oxide are dissolved in 5 mL of EtOH then an ethanoic solution of $NaCH_3S$ (182 mg) was added. The suspension was stirred under reflux for 1h, cooled at room temperature and filtered. The filtrate is diluted with water and extracted with 4×20 mL of Et_2O. Finally the residue is purified on alumina chromatography using a 3:1 CH_2Cl_2/MeCN eluent to give a colorless powder (yield: 275mg, 75%). ^{1}H NMR: 2.94 (3H, s); 7.68 (1H, dd), 8.09 (2H,m), 8.51 (1H, dt) in DMSO d6.

N-Oxy-pyridine-4-carbodithioic Acid Methyl Ester (L2): This ligand was obtained according to the reported experimental procedure.[35]

Complexes synthesis: Compound **1** was obtained using the following procedure: 0.1 mmol of 3-methylsulfanyl-pyridine N-oxide (**L1**) was dissolved in 10ml of $CHCl_3$ and added drop by drop to a 10 ml $CHCl_3$ solution of 0.1 mmol of $[Dy(hfac)_3(H_2O)_2]$. The resulting solution was stirred at room temperature for five minutes and covered by a layer of n-heptane. After storing at 2°C for several days single crystal suitable for X-ray diffraction were obtained. The same procedure was used for the synthesis of **2**.

4. Results and discussion

4.1. Crystal structure description

Single-crystal X-ray diffraction measurement on **1** reveals that it crystallizes in monoclinic $P2_1/n$ space group. The main structural parameters are listed in Table S1.

The asymmetric unit of the compound is made of one Dy^{III} ion, three $hfac^-$ ligands and one 3-methylsulfanyl-pyridine N-oxide ligand (**L1**). Its oxygen atom (O7) links two Dy^{III} ions in a μ_2 mode (Figure 1a). A center of inversion is located in the middle of the double bridge and makes the two Dy^{III} ions equivalent. The Dy-Dy distance is 4.02(8) Å. Each Dy^{III} is eight coordinated by six oxygen atoms (O1, O2, O3, O4, O5 and O6) from $hfac^-$ ligands and two oxygen atoms (O7) from **L1**.

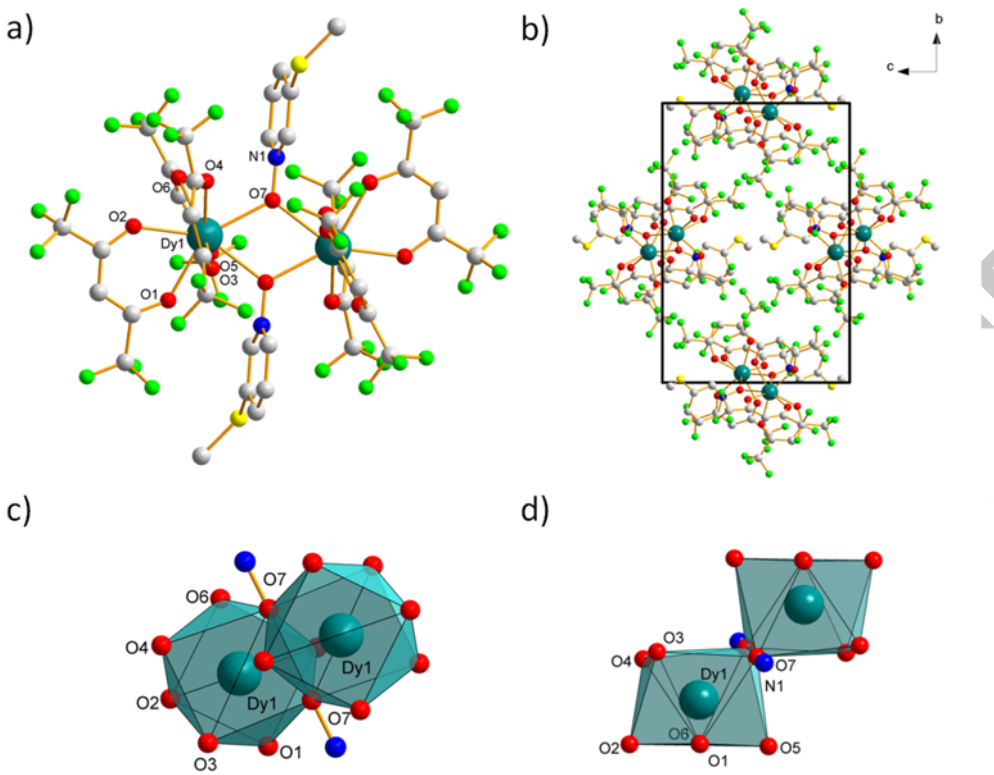

Figure 1. (a) Representation of **1** (dysprosium, dark green; fluorine, light green; sulfur, yellow; oxygen, red; carbon, grey) . (b) View of the crystal packing along a axis. (c) and (d) different views of the coordination environment of the Dy^{III} atom.

The bond lengths of Dy-$O_{(hfac-)}$ are in the range 2.32(6)-2.37(2) Å, while Dy-$O_{(L1)}$ are 2.38(3) Å (Table S2). CSM analysis [36, 37] shows that the coordination environment of the Dy^{III} ion is very close to a square antiprism (D_{4d}) geometry (CSM = 0.618) (Figures 1c and 1d and Table S3). The two planes of the square antiprism are made of O1, O2, O5, O6 and O3, O4, O7, O7 atoms, respectively. Each dimer is well isolated and the shortest interdimer Dy-Dy distance is 11.17(9) Å (Figure 1b).

Single-crystal X-ray measurement on **2** highlights that it crystallizes in triclinic *P-1* space group. The main structural parameters are listed in Table S4. The substitution of **L1** for 4-methylcarbodithioate-pyridine N-oxide (**L2**) in the coordination process affords a very similar dimer (Figure 2).

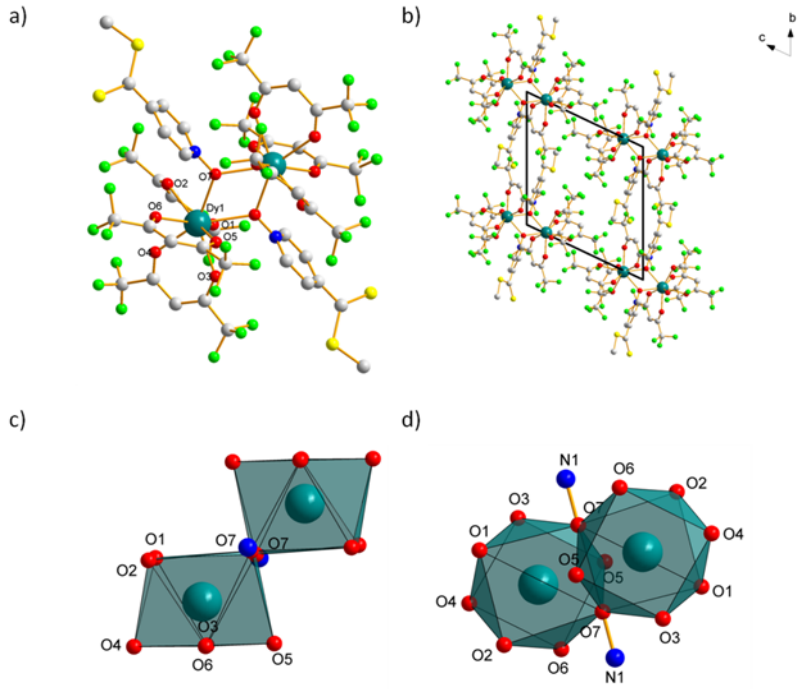

Figure 2. (a) Representation of **2** (dysprosium, dark green; fluorine, light green; sulfur, yellow; oxygen, red; carbon, grey). (b) View of the crystal packing along a axis. (c) and (d) different views of the coordination environment of the Dy^{III} atom.

Similar coordination modes are observed, as well as similar intradimer Dy-Dy distances (4.05(2) Å, see Table S5 for distances and angles), and similar coordination polyhedron (square antiprism). CSM factor is only slightly lower (CSM = 0.345) indicating an even more symmetric D_{4d} environment in **2** (Table S6). Overall the only noticeable difference is the shortest interdimer Dy-Dy distance that is smaller on **2** (Dy-Dy = 9.08(7) Å).

TGA/DSC analyses (Figure S2) clearly demonstrate that both complexes are stable to at least 200°C and have very good sublimation properties (90% brutal weight loss) that make them suitable for surface deposition. This is a very similar behavior to the one of **DyPyNO** that has permitted its controlled deposition on surfaces. [15, 18]

4.2. Magnetic measurements

Static and dynamic magnetic susceptibility measurements were performed on polycrystalline samples of **1** and **2** embedded in grease. The room temperature values of the $\chi_M T$ products are 26.38 and 27.23 emu.K.mol^{-1} at 300 K, for **1** and **2**, respectively. This is slightly lower than the expected 28.34 emu.K.mol^{-1} for two isolated

Dy^{III} ions.[38] The curves decrease as the temperature is lowered because of the progressive depopulation of the m_J levels of the J = 15/2 multiplet of the Dy^{III} [38] and/or because of intramolecular Dy-Dy antiferromagnetic interaction as highlighted on related compounds (Figure S3). [14-18, 39, 40]

Ab-initio calculations confirm these findings. In the frame of the effective spin S = 1/2, antiferromagnetic Dy-Dy coupling is found to be J_{total} = -2.65 cm^{-1} and -2.99 cm^{-1} for **1** and **2**, respectively. These values are obtained by considering the relative angles and distances between the molecular anisotropy axes as shown on Figure 3 (dipolar contribution, J_{dip}) [41] and the magnetic interaction computed (exchange contribution, J_{exch}).[17] For **1** values decompose as $J_{total} = J_{dip} + J_{exch}$ = -2.52 - 0.125 cm^{-1} and for **2**, $J_{total} = J_{dip} + J_{exch}$ = -2.49 - 0.50 cm^{-1}. These values as well as the orientation of the easy magnetic axes are close to what obtained on **DyPyNO** ($J_{total} = J_{dip} + J_{exch}$ = -2.44 - 0.25 = -2.69 cm^{-1}) and similar dimers. [14, 17, 42-45]

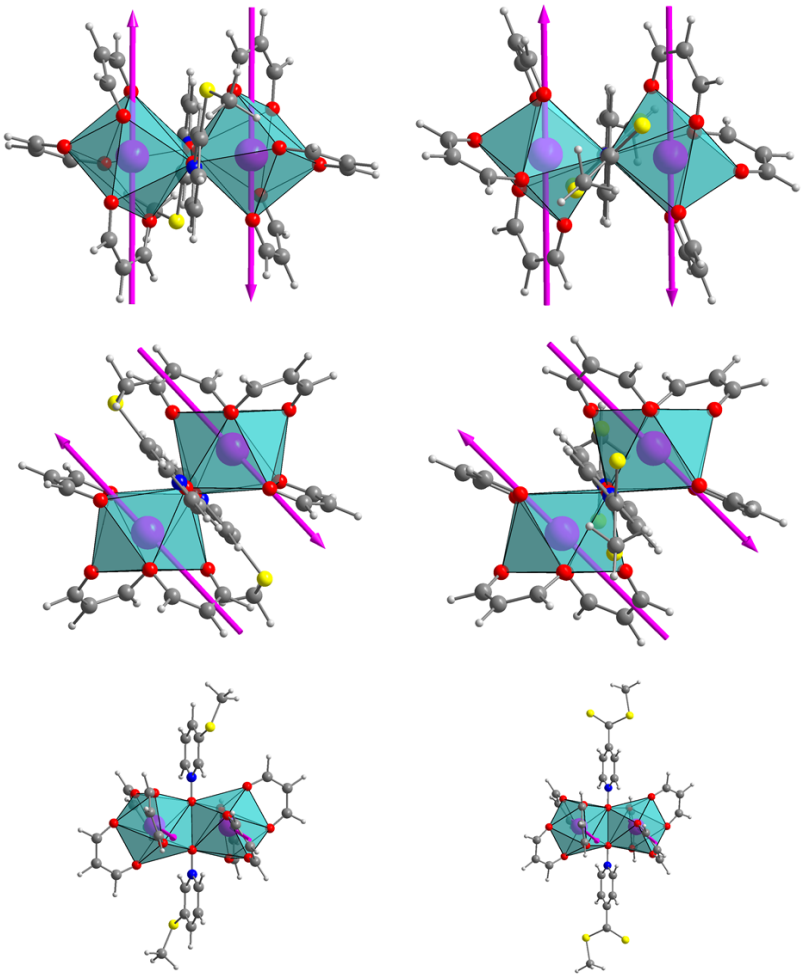

Figure 3. Representation of the easy magnetic axes on various orientation of **1** (left) and **2** (right).

Dynamic magnetic behavior was investigated from 1.8 K to 14 K in the 0.1-1500 Hz frequency range in the absence of external field. Strong frequency dependence of the in-phase (χ_M') and out-of-phase (χ_M") component of the magnetization is observed (Figures 4-5, S4-S5).

The relaxation times τ were extracted by fitting χ_M" vs frequency curves (values in Tables S7-S8) using an extended Debye model. The Arrhenius plot (ln(τ) vs T^{-1}) is reported in Figure 6. Two main regimes can be evidenced. A thermally activated relaxation (Orbach-like relaxation, with $\tau = \tau_0 \exp(-\Delta/kT)$), above 10K and a temperature-independent one (quantum tunneling-like relaxation with $\tau = \tau_{tunneling}$) below 2K. Any attempts to consider other relaxation modes failed as over-parametrization occurs. [46] It is worth noting that on **DyPyNO** pure Orbach relaxation was found only above 15K using very high frequencies (10-70kHz). In this study, we use a conventional ac susceptometer and we were not able to isolate such a pure relaxation regime. However it can be clearly seen from Figure 6 that the thio-substitution (compounds **1** and **2**) of the bare dimer (**DyPyNO**) does not damage the energy barrier for spin reversal at high temperature. At low temperature, the temperature-independent regime is affected and $\tau_{tunneling}$ = 0.07 and 0.04s are observed on **1** and **2**, respectively (0.38s on **DyPyNO**).

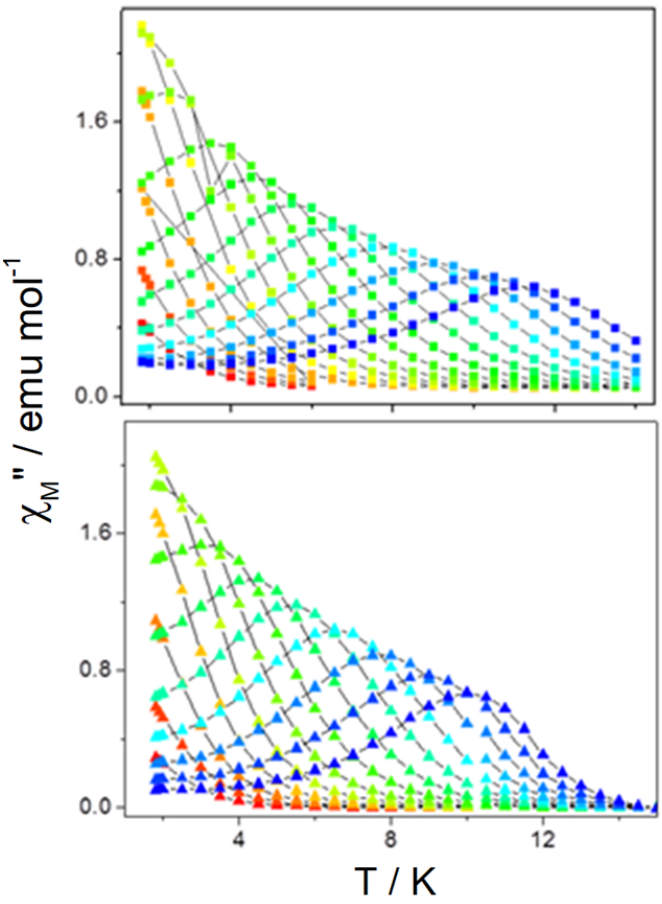

Figure 4. Temperature dependence of the out-of-phase component of the magnetization measured in absence of external static field on **1** (top) and **2** (bottom) for frequencies ranging from 1 to 1500 Hz (form red to blue).

The distribution of the relaxation times τ can be extracted from the Cole-Cole plots of the in-phase and out-of phase components of the magnetization that were normalized over the isothermal susceptibility (χ_T) (Figure S6 and Tables S9-S10). This allows estimating α, considering that α = 0 for a single relaxation time (perfect SMM) up to α = 1 for an infinity of relaxation times (spin glass). The highest α values are 0.23 and 0.27 for **1** and **2**, respectively, suggesting a relatively narrow distribution of the relaxation times. The relaxing fractions are 91% and 97% for **1** and **2**. In the high temperature region (T = 10K), α is as low as 0.15 and 0.08 for **1** and **2**. This confirms that the dimers tend to adopt an almost pure relaxation process in this temperature region. Relaxing fractions are still very good (90% and 80% for **1** and **2**).

Overall, we recall that on a structural point of view the only significant differences between the two derivatives are a weak intermolecular Dy-Dy distance

change (9.08(7) Å in **2** and 11.17(9) Å in **1**) and slight symmetry change of the environment of the Dy^{III} ion (CSM = 0.345 for **2** and 0.618 for **1**). On the static magnetic point of view the Dy-Dy distance change is too weak to induce any sizeable variation in the total exchange value, J_{total}, via its dipolar component, J_{dip}.

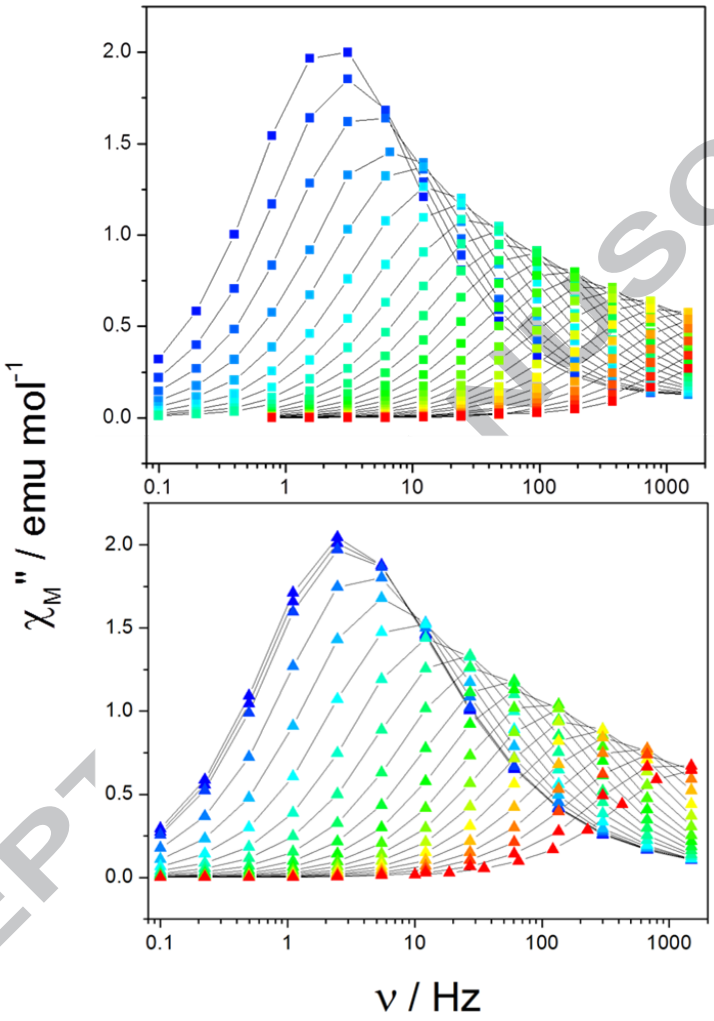

Figure 5. Frequency dependence of the out-of-phase component of the magnetization measured in absence of external static field on **1** (top) and **2** (bottom) for temperatures ranging from 1.8 to 14K (blue to red).

Only weak change is seen on the low temperature relaxation time that diminish as the coordination environment of the Dy^{III} get more symmetric when passing from **1** to **2**.

This counter-intuitive conclusion is however in agreement with recent findings that highlight that the coordination symmetry around a given lanthanide ion is not the main factor that governs its relaxation. Indeed both electrostatic contribution [22, 47-49]

(especially its quadrupolar expansion) and spin-phonon coupling are much more relevant in tailoring the magnetic behavior of lanthanide-based SMM. [50] Consequently, one can say that the two different thio-substitutions on the pyridine ligand modify, but in a reasonable way, the magnetic features of the original dimer **DyPyNO**. The low temperature $\tau_{tunneling}$ is slightly diminished but high temperature energy barrier seems to be preserved in the investigated frequency range. This offers the possibility to test both derivatives for surface deposition with a reasonable success. Consequently we are confident that **1** and **2** could be suitable derivatives for surface grafting.

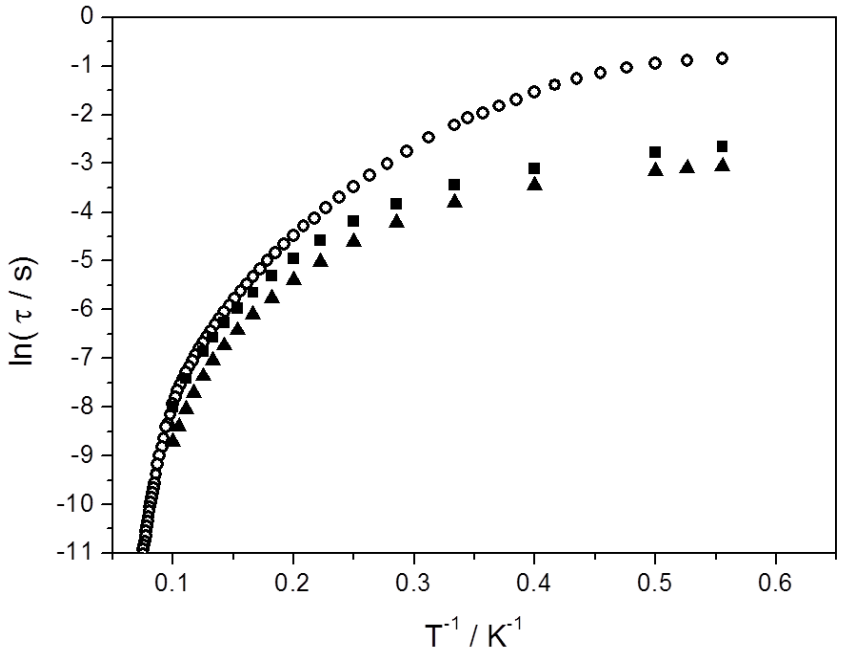

Figure 6. Representation of the relaxation times measured on **1** (squares) and **2** (triangles) and comparison with the already reported compound **DyPyNO** (circles).[12]

Conclusions

In conclusion we report here, two derivatives (**1** and **2**) of a well-known SMM, (**DyPyNO)**, targeted to be deposited on gold surfaces. The substitution of the pyridine ring by the anchoring groups fulfills our objectives and very slightly modifies dimer's SMM properties. Almost no differences were found in the two substitutions; this highlights the magnetic robustness of the Dy^{III} core of these dimers. Indeed, given the different geometries of the anchoring groups in **1** and **2** it would be interesting to

investigate their surface deposition ability on gold. We are currently testing these possibilities.

Conflicts of interest

There are no conflicts to declare.

Acknowledgments

We acknowledge financial support from INSA Rennes, CNRS, Université de Rennes 1, Region Bretagne, Rennes Métropole, China Scholarship Council (CSC) and the Agence Nationale de la Recherche (ANR-13-BS07-0022-01). Thierry Guizouarn and Thierry Roisnel are acknowledged for their assistance on magnetic and single-crystal diffraction measurements, respectively. K.B. acknowledges Institut Universitaire de France (IUF). B. L. G. thanks the GENCI/IDRIS-CINES Centre in France for high-performance computing resources.

Supplementary information

Additional structural and magnetic data can be found in supplementary material.

CCDC 1819460 and CCDC 1819461 contains the supplementary crystallographic data for **1** and **2**, respectively. These data can be obtained free of charge via http://www.ccdc.cam.ac.uk/conts/retrieving.html, or from the Cambridge Crystallographic Data Centre, 12 Union Road, Cambridge CB2 1EZ, UK; fax: (+44) 1223-336-033; or e-mail: deposit@ccdc.cam.ac.uk.

Notes and references

[1] C. Benelli, D. Gatteschi, Introduction to Molecular Magnetism: From Transition Metals to Lanthanides, Wiley, 2015.

[2] D. Gatteschi, R. Sessoli, J. Villain, Molecular Nanomagnets, Oxford University Press, Oxford, 2006.

[3] M. Verdaguer, J.-P. Launay, Electrons in Molecules; From Basic Principles to Molecular Electronics, Oxford University Press, 2013.

[4] H. Kronmuller, S. Parkin, Handbook of Magnetism and Advanced Magnetic Materials, 5 Volume Set.
[5] C.A.P. Goodwin, F. Ortu, D. Reta, N.F. Chilton, D.P. Mills, Nature, 548 (2017) 439-442.
[6] F.-S. Guo, B.M. Day, Y.-C. Chen, M.-L. Tong, A. Mansikkamäki, R.A. Layfield, Science, 362 (2018) 1400-1403.
[7] J. Dreiser, J. Phys.-Condens. Matter, 27 (2015) 183203.
[8] T. Ladnorg, A. Welle, S. Heißler, C. Wöll, H. Gliemann, Beilstein J. Nanotechnol., 4 (2013) 638-648.
[9] M. Mannini, L. Sorace, L. Gorini, F.M. Piras, A. Caneschi, A. Magnani, S. Menichetti, D. Gatteschi, Langmuir, 23 (2007) 2389-2397.
[10] V. Lanzilotto, L. Malavolti, S. Ninova, I. Cimatti, L. Poggini, B. Cortigiani, M. Mannini, F. Totti, A. Cornia, R. Sessoli, Chem. Mat., (2016).
[11] A. Cornia, M. Mannini, Single-Molecule Magnets on Surfaces, in: Molecular Nanomagnets and Related Phenomena, Springer Berlin Heidelberg, 2014, pp. 1-38.
[12] M. Perfetti, F. Pineider, L. Poggini, E. Otero, M. Mannini, L. Sorace, C. Sangregorio, A. Cornia, R. Sessoli, Small, (2013) 323-329.
[13] M. Mannini, F. Pineider, C. Danieli, F. Totti, L. Sorace, P. Sainctavit, M.A. Arrio, E. Otero, L. Joly, J.C. Cezar, A. Cornia, R. Sessoli, Nature, 468 (2010) 417-421.
[14] X. Yi, K. Bernot, F. Pointillart, G. Poneti, G. Calvez, C. Daiguebonne, O. Guillou, R. Sessoli, Chem.-Eur. J., 18 (2012) 11379-11387.
[15] E. Kiefl, M. Mannini, K. Bernot, X. Yi, A. Amato, T. Leviant, A. Magnani, T. Prokscha, A. Suter, R. Sessoli, Z. Salman, ACS Nano, 10 (2016) 5663-5669.
[16] X. Yi, G. Calvez, C. Daiguebonne, O. Guillou, K. Bernot, Inorg. Chem., 54 (2015) 5213-5219.
[17] G. Huang, X. Yi, J. Jung, O. Guillou, O. Cador, F. Pointillart, B. Le Guennic, K. Bernot, Eur. J. Inorg. Chem., (2018) 326-332.
[18] I. Cimatti, X. Yi, R. Sessoli, M. Puget, B.L. Guennic, J. Jung, T. Guizouarn, A. Magnani, K. Bernot, M. Mannini, Appl. Surf. Sci., 432 (2018) 7-14.
[19] X. Yi, J. Shang, L. Pan, H. Tan, B. Chen, G. Liu, G. Huang, K. Bernot, O. Guillou, R.-W. Li, ACS Appl. Mater. Interfaces, 8 (2016) 15551–15556.
[20] M. Li, H. Wu, Q. Yang, H. Ke, B. Yin, Q. Shi, W. Wang, Q. Wei, G. Xie, S. Chen, Chem. Eur. J., 23 (2017) 17775-17787.
[21] P. Zhang, J. Jung, L. Zhang, J. Tang, B. Le Guennic, Inorg. Chem., 55 (2016) 1905-1911.
[22] N.F. Chilton, D. Collison, E.J.L. McInnes, R.E.P. Winpenny, A. Soncini, Nat Commun, 4 (2013) 2551.
[23] S. Gómez-Coca, D. Aravena, R. Morales, E. Ruiz, Coord. Chem. Rev., 289–290 (2015) 379-392.
[24] Y.-S. Xue, J.-C. Bian, M.-M. Wu, P.-Y. Cheng, W.-M. Wang, Z.-L. Wu, M. Fang, Polyhedron, 138 (2017) 306-311.
[25] K. Zhang, C. Yuan, F.-S. Guo, Y.-Q. Zhang, Y.-Y. Wang, Dalton Trans., 46 (2017) 186-192.
[26] Y.-L. Wang, C.-B. Han, Y.-Q. Zhang, Q.-Y. Liu, C.-M. Liu, S.-G. Yin, Inorg. Chem., 55 (2016) 5578-5584.
[27] Y. Peng, V. Mereacre, A. Baniodeh, Y. Lan, M. Schlageter, G.E. Kostakis, A.K. Powell, Inorg. Chem., (2015) 68-74.
[28] W.-Y. Zhang, P. Chen, H.-F. Li, Y.-Q. Zhang, P.-F. Yan, W.-B. Sun, Chemistry – An Asian Journal, 13 (2018) 1725-1734.
[29] M. Guo, Y. Xu, J. Wu, L. Zhao, J. Tang, Dalton Trans., 46 (2017) 8252-8258.
[30] S.-Y. Lin, J. Wu, C. Wang, L. Zhao, J. Tang, Eur. J. Inorg. Chem., 2015 (2015) 5488-5494.
[31] A. Altomare, M.C. Burla, M. Camalli, G.L. Cascarano, C. Giacovazzo, A. Guagliardi, A.G.G. Moliterni, G. Polidori, R. Spagna, J. Appl. Crystallogr., 32 (1999) 115-119.
[32] L. Farrugia, J. Appl. Crystallogr., 32 (1999) 837-838.
[33] L.J. Farrugia, J. Appl. Crystallogr., 45 (2012) 849-854.

[34] K. Bernot, L. Bogani, A. Caneschi, D. Gatteschi, R. Sessoli, J. Am. Chem. Soc., 128 (2006) 7947-7956.
[35] I. Abrunhosa, M. Gulea, S. Masson, Synthesis, 2004 (2004) 928-934.
[36] S. Alvarez, P. Alemany, D. Casanova, J. Cirera, M. Llunell, D. Avnir, Coord. Chem. Rev., 249 (2005) 1693-1708.
[37] S. Alvarez, Dalton Trans., (2005) 2209-2233.
[38] O. Kahn, Molecular Magnetism, Wiley-VCH, Weinheim, 1993.
[39] F. Pointillart, Y. Le Gal, S. Golhen, O. Cador, L. Ouahab, Chem. Eur. J., 17 (2011) 10397-10404.
[40] C.Y. Chow, H. Bolvin, V.E. Campbell, R. Guillot, J.W. Kampf, W. Wernsdorfer, F. Gendron, J. Autschbach, V.L. Pecoraro, T. Mallah, Chem. Sci., 6 (2015) 4148-4159.
[41] X. Yi, K. Bernot, O. Cador, J. Luzon, G. Calvez, C. Daiguebonne, O. Guillou, Dalton Trans., 42 (2013) 6728-6731.
[42] W.-Y. Zhang, Y.-M. Tian, H.-F. Li, P. Chen, W.-B. Sun, Y.-Q. Zhang, P.-F. Yan, Dalton Trans., 45 (2016) 3863-3873.
[43] X. Zhang, N. Xu, W. Shi, B.-W. Wang, P. Cheng, Inorg. Chem. Front., 5 (2018) 432-437.
[44] H.-R. Tu, W.-B. Sun, H.-F. Li, P. Chen, Y.-M. Tian, W.-Y. Zhang, Y.-Q. Zhang, P.-F. Yan, Inorg. Chem. Front., (2017).
[45] J. Long, F. Habib, P.H. Lin, I. Korobkov, G. Enright, L. Ungur, W. Wernsdorfer, L.F. Chibotaru, M. Murugesu, J. Am. Chem. Soc., 133 (2011) 5319-5328.
[46] S.T. Liddle, J. van Slageren, Chem. Soc. Rev., 44 (2015) 6655-6669.
[47] P.-P. Cen, S. Zhang, X.-Y. Liu, W.-M. Song, Y.-Q. Zhang, G. Xie, S.-P. Chen, Inorg. Chem., 56 (2017) 3644-3656.
[48] W.-B. Sun, P.-F. Yan, S.-D. Jiang, B.-W. Wang, Y.-Q. Zhang, H.-F. Li, P. Chen, Z.-M. Wang, S. Gao, Chem. Sci., (2016) 684-691.
[49] J. Jung, F. Le Natur, O. Cador, F. Pointillart, G. Calvez, C. Daiguebonne, O. Guillou, T. Guizouarn, B. Le Guennic, K. Bernot, Chem. Commun., 50 (2014) 13346-13348.
[50] A. Lunghi, F. Totti, S. Sanvito, R. Sessoli, Chem. Sci., 8 (2017) 6051-6059.

Anchorable derivatives of the well-known Single-Molecule Magnets (SMMs) **DyPyNO** are reported. The SMM behaviors of these derivatives are remarkably well-preserved upon the thio-substitution and offers good possibilities to graft these SMMs on surface.

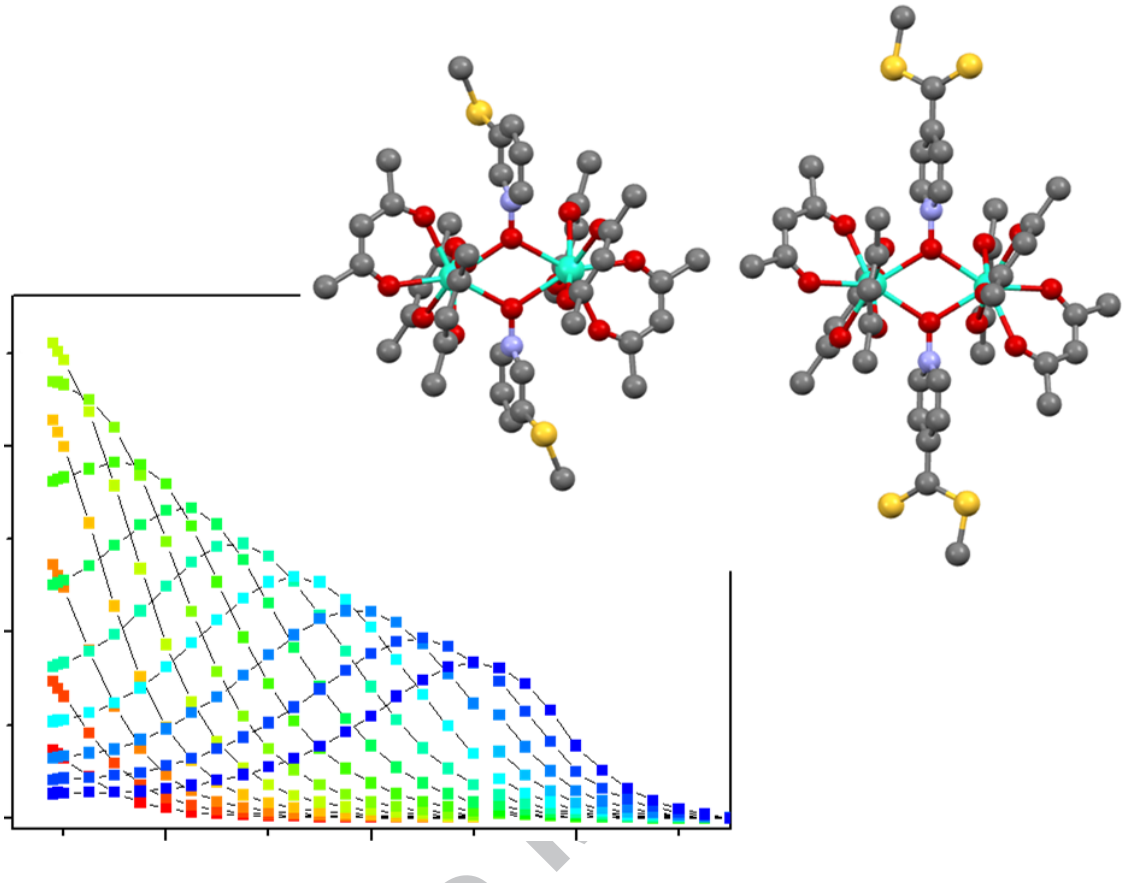

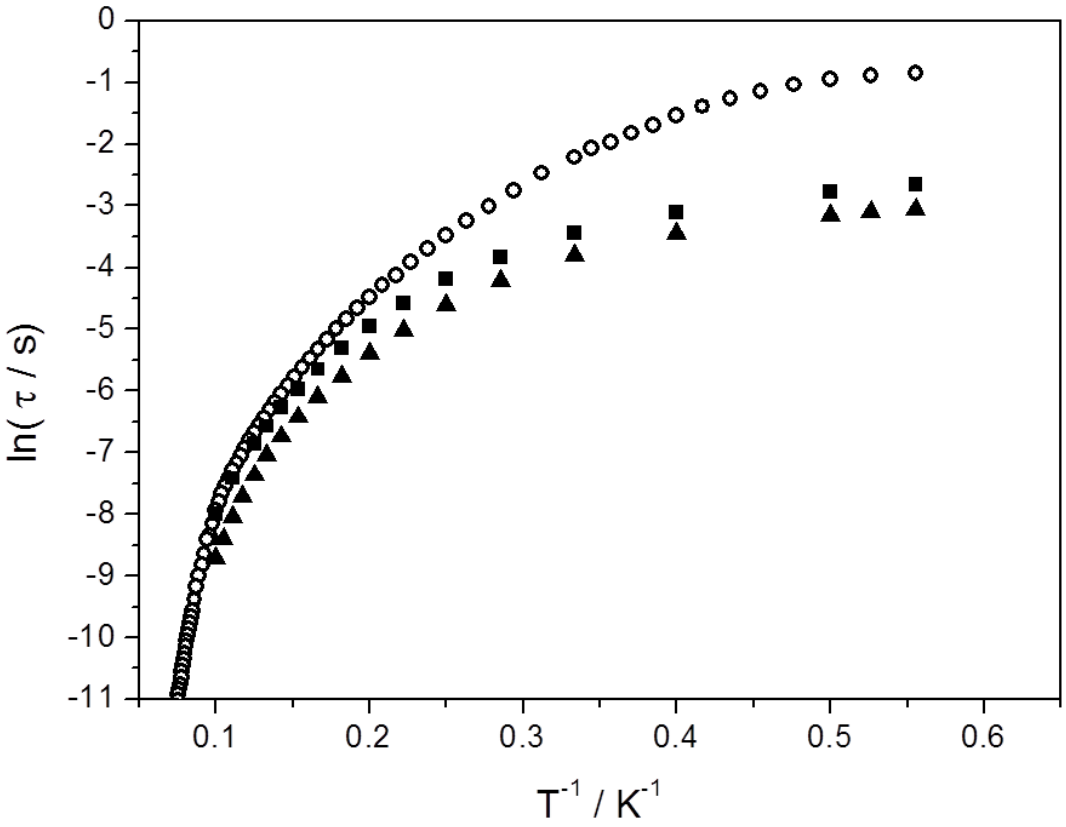
0
-1
-2
-3
-4
-5
-6
-7
-8
-9
-10
-11
ln(τ / s)
0.1
0.2
0.3
0.4
0.5
0.6
T-1 / K-1

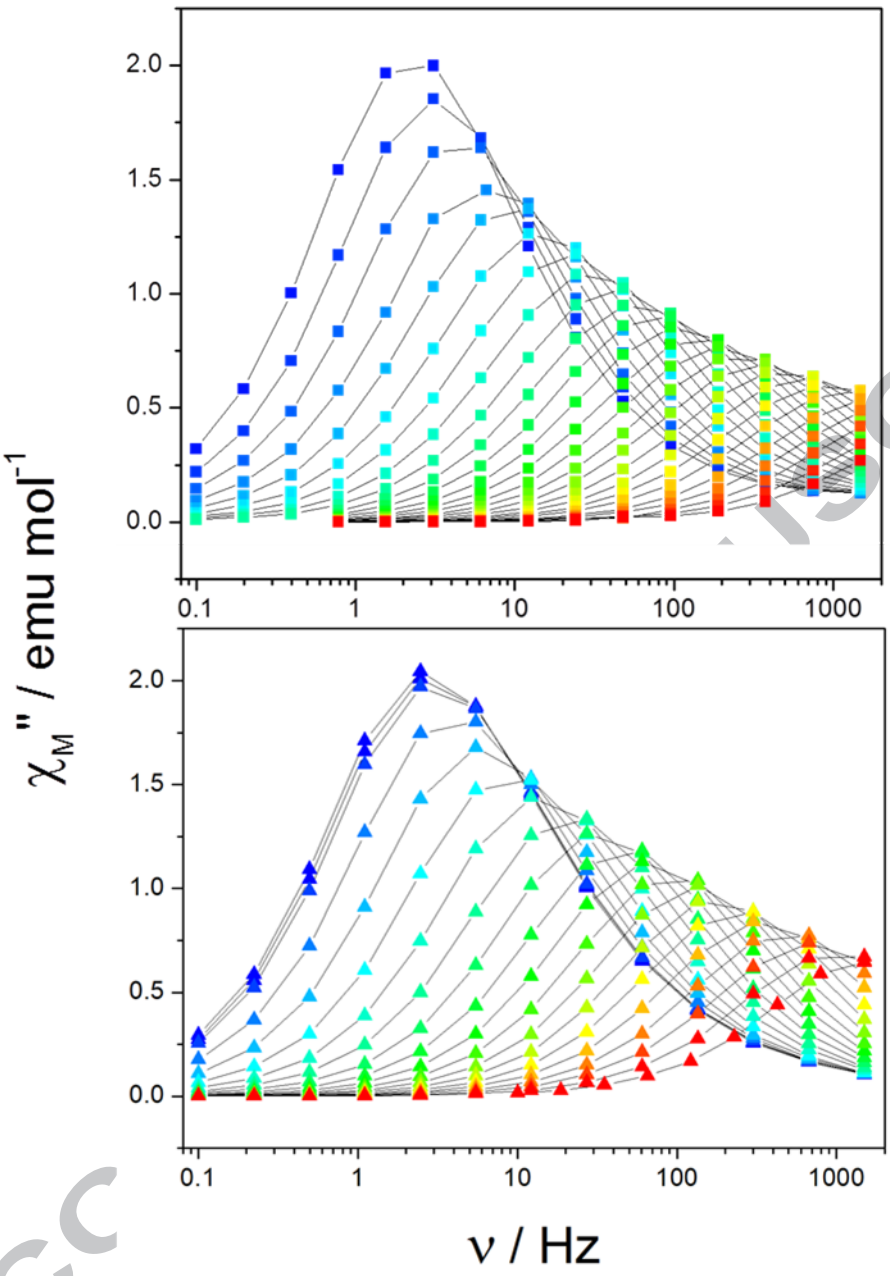

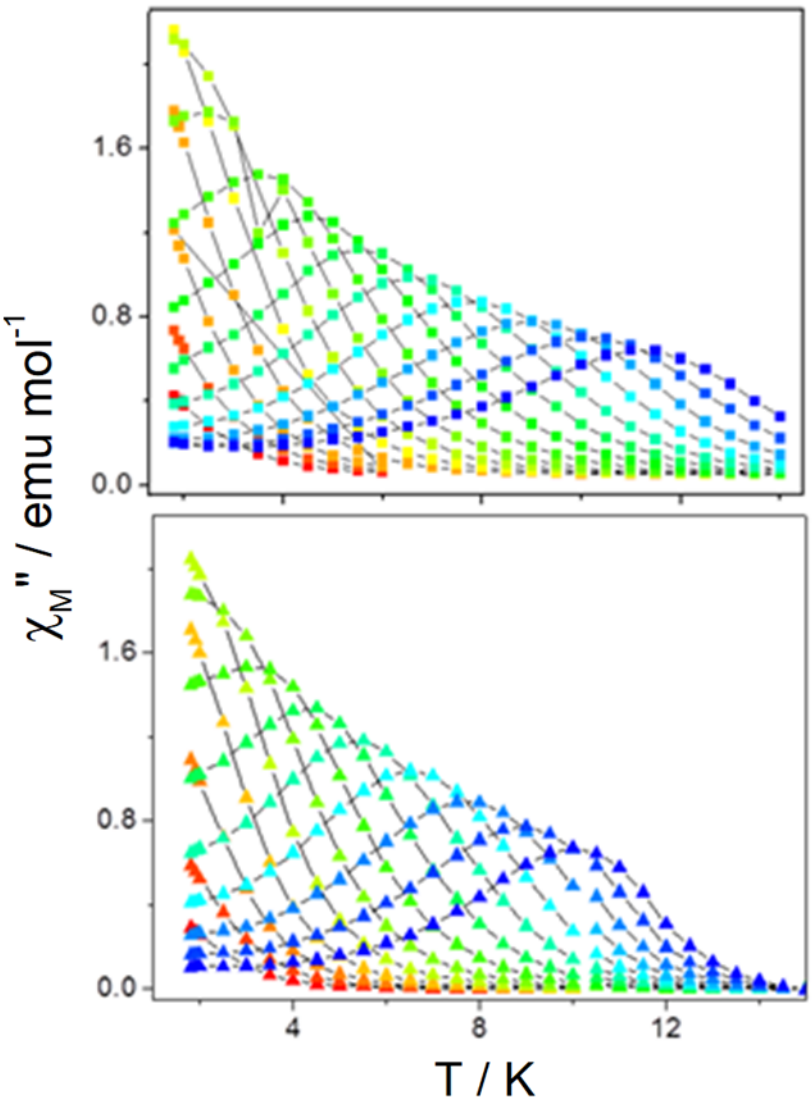

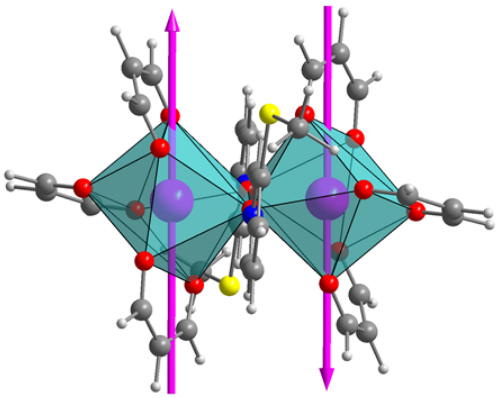

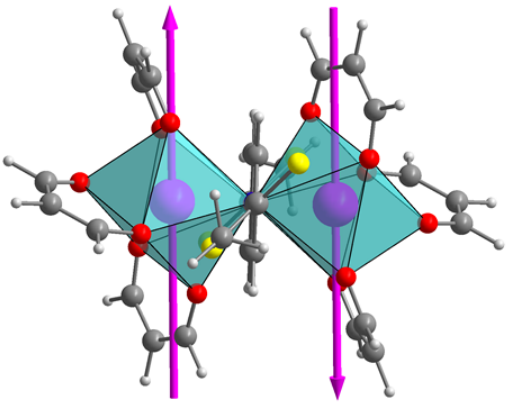

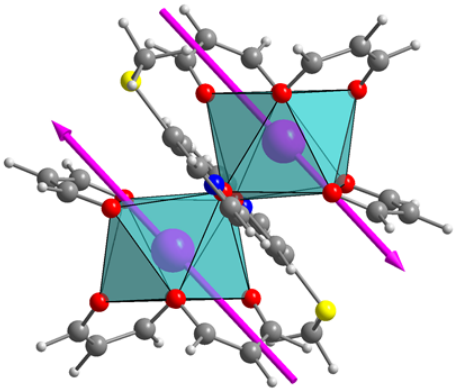

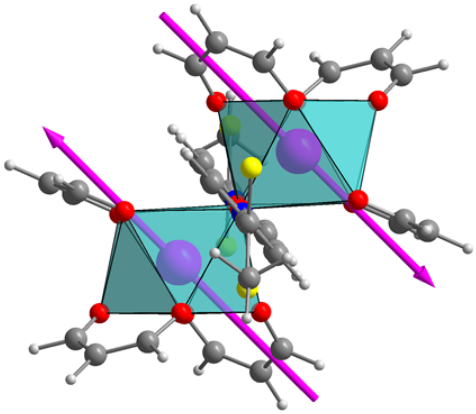

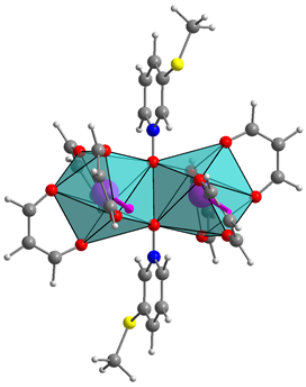

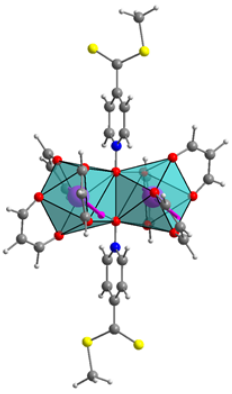

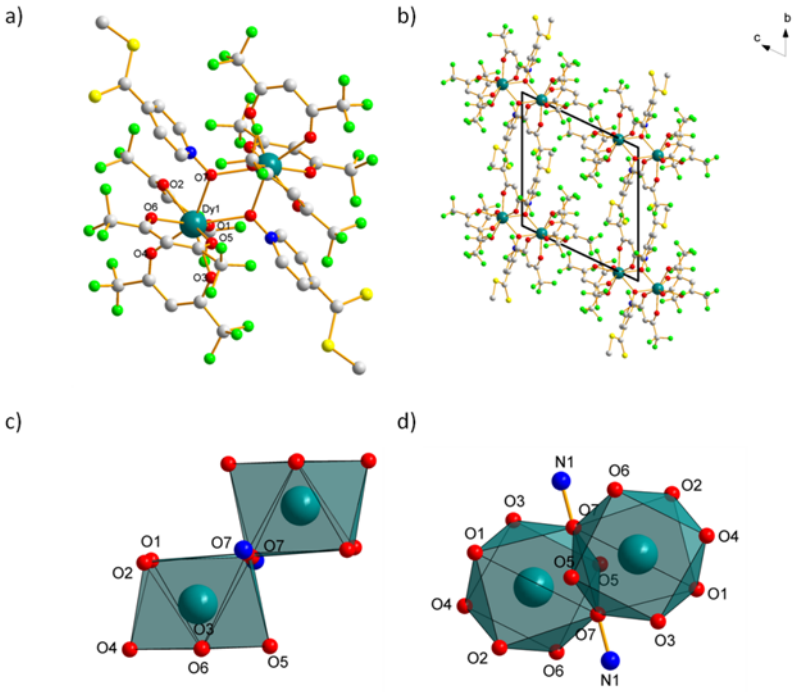
a)
b)
c)
d)
O1
O2
O3
O4
O5
O6
O7
Dy1
N1
b
c

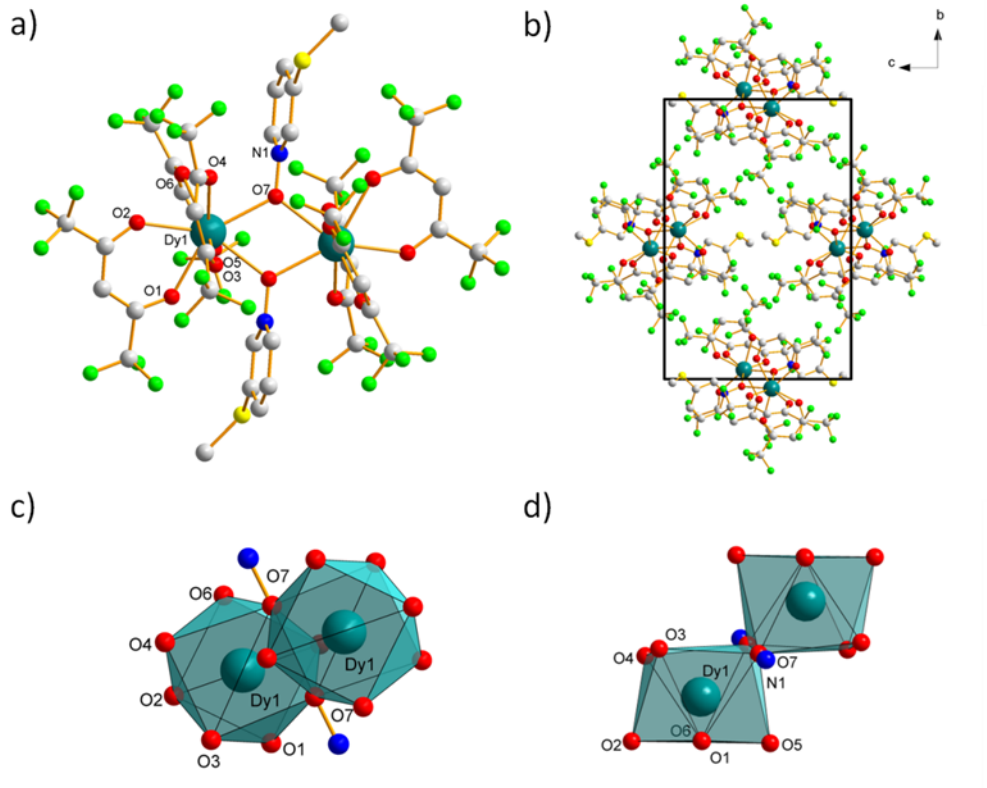
a)
b)
c)
d)
O1
O2
O3
O4
O5
O6
O7
Dy1
N1
b
c

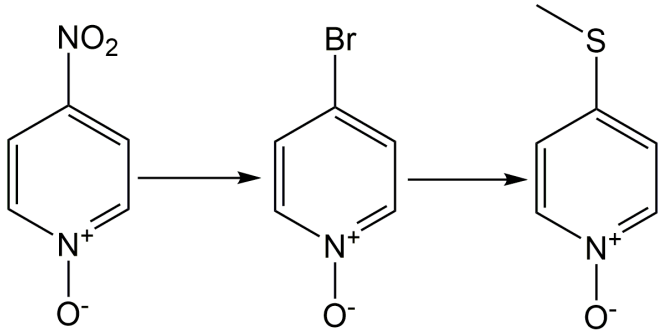

(**L1**)

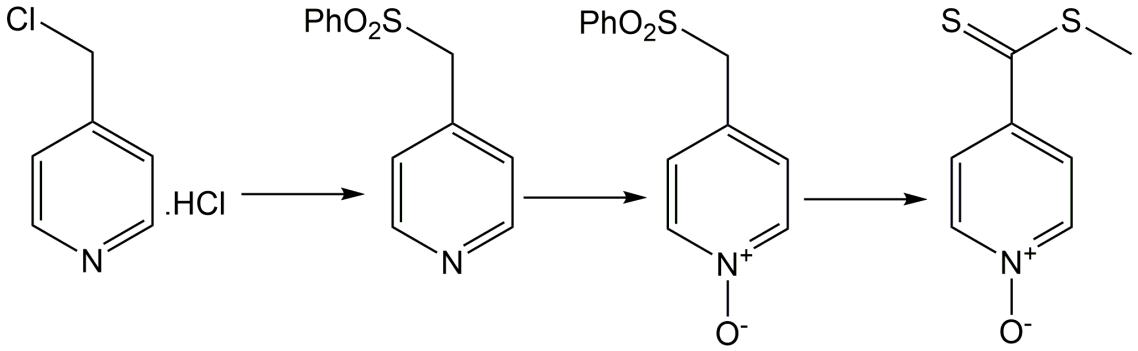

(**L2**)